



# Improving strength of composite waste polyethylene terephthalate (PET) plastics wall cladding through reinforcing with waste tire steel fibers

Peter Laurian<sup>1</sup> · Duwa Hamisi Chengula<sup>1</sup> · Patrice Nyangi<sup>1</sup>

Received: 29 April 2025 / Accepted: 22 August 2025  
© Springer Nature Switzerland AG 2025

## Abstract

Traditional wall cladding materials such as natural stone (marble and granite), composite panels (porcelain and ceramic), metals (stainless steel to copper), and glass are typically too expensive for medium and low-income households in Tanzania. For instance, ceramic tiles in Tanzania, as reported by CTM Tanzania (a leading specialist retailer), cost approximately TZS 28,000 to 118,055.56 (USD 10.58 to 44.86) per square meter, typically higher than the approximately TZS 10,000 (USD 3.78) per square meter for locally produced composite wall cladding. This study investigated the potential of developing an affordable and sustainable alternative utilizing recycled PET plastic, sand, and steel fibers. The aim was to minimize construction costs and reduce waste by recycling non-biodegradable PET. To achieve this, laboratory experiments were conducted to investigate the physical and mechanical properties of composites made from hot-blended PET plastic, sand, and recycled steel fibers. The density of composites, formulated with a constant PET-sand ratio and varying recycled steel fiber content, was directly associated with fiber concentration, increased from 1.622 g/cm<sup>3</sup> (0% fibers) to 2.852 g/cm<sup>3</sup> (5% fibers). Water absorption exhibited an interesting pattern: it initially decreased from 0.84% (0% fibers) to 0.65% (2% fibers), then rose dramatically from 1.8% (2.5% fibers) to 4.7% (5% fibers). The highest compressive strength, 22.8 MPa, was achieved by a specimen containing 3% steel fibers. Additionally, impact tests exhibited the incorporation of 1–5% fiber content improving the material's toughness, and enhancing stiffness. Petrographic analysis confirmed the even distribution of steel fibers within the matrix, which contributed to their increased strength. Based on the findings, an optimal composition of 1:1 PET-sand ratio, with steel fiber contents ranging from 2 to 3.5% is recommended for developing composite wall cladding materials. This mixture provides excellent mechanical properties and low water absorption. By repurposing these waste materials for wall cladding, we can mitigate environmental concerns and encourage eco-friendly construction, while providing a more affordable option for building projects. Further research is required, particularly regarding the scalability of production and long-term performance in various environmental conditions.

**Keywords** Waste steel fibers · PET waste plastic · Wall cladding · Waste tires · Compressive strength · Impact strength

## Introduction

Plastic is a synthetic or semi-synthetic organic compound that can be molded when heated. Common types of plastics include polyethylene, polypropylene, polyvinyl chloride, polyethylene terephthalate, and polystyrene [1, 2]. Plastic has become an essential part of modern life, having a wide range of applications including packaging [3]. The packaging industry absorbs the highest quantity of plastics generated globally and is among the main causes of waste plastics in the environment [4]. Per capita plastic waste generation is around 5.6 kg/year, with approximately 315 thousand tons

---

✉ Peter Laurian  
peterlaurian@gmail.com

Duwa Hamisi Chengula  
chengula@yahoo.com

Patrice Nyangi  
patrice.mkono@must.ac.tz

<sup>1</sup> Department of Civil Engineering, College of Engineering and Technology, Mbeya University of Science and Technology, P.O. Box 131, Mbeya, Tanzania

of plastic waste generated in Tanzania per year [5]. Plastics are relatively durable and lightweight materials with thermal and electrical insulation characteristics [6]. The extensive use of plastics has generated a substantial amount of plastic waste, leading to harmful environmental impacts. If not managed appropriately, these challenges can cause landfill congestion, environmental pollution, and addition to climate change. Sustainable management strategies for plastic waste, especially in urban towns, are essential; these include thermal breakdown, landfills, mechanical pulverisation, incineration, and microbiological decomposition. The environmentally friendly and sustainable approach is to recycle plastic waste for construction purposes. Research into innovative applications of recycling plastic waste for construction use can help minimize environmental impact, identify alternative materials, and reduce the cost of construction [7].

Polyethylene Terephthalates (PET) are among the widely used plastics found in numerous applications, including beverage bottles, packaging, clothing, and carpeting. They are relatively inexpensive, lightweight, and durable materials that have the potential of being recycled into various products with a wide range of applications [8]. PET plastic bottles rule the market for water packaging, but their common use creates a substantial threat to human health and ecosystems. The discharge of great volumes of PET plastic bottles into the environment raises concerns regarding environmental protection. As a result, there is an urgent need to create and execute effective recovery technologies [9]. Recycling is a valuable method for reducing the accumulation of PET plastic waste bottles in landfills and the environment. By recycling PET bottles to innovate construction materials, it can provide a low-cost and sustainable alternative to construction materials while reducing the disposal of waste in landfills [10].

Plastic waste provides significant potential for use in construction materials, as binders, coarse aggregate, fine aggregate, modifiers, or replacement for cement and sand in the manufacturing of bricks, tiles, concrete, and roads [11]. Particularly, studies have explored the potential use of PET plastics as binders in numerous composite materials. For instance, PET plastics were successfully applied as a binder to develop bathroom wall composite materials when integrated with cocoa hull powder [12]. Research on roof tiles cast with plastic waste as binding material revealed that 40% plastic waste yields optimal physical and mechanical properties [13]. Similarly, an experimental study on roof tile production utilizing waste PET and river sand found that 40% and 50% PET waste plastic produced favorable results [14]. The highest compressive strength in roof tiles developed from waste plastic, sand, and fly ash was achieved with 50% PET waste plastic [15]. Furthermore,

characterization of floor tile composites exhibited optimal compressive strength and water absorption with 44.44% PET waste plastic and 55.56% sand content [16]. Previous characterization studies, such as one by [17] on hot-mixed PET waste plastic and sand, revealed that a matrix of 50% PET waste plastic and 50% sand offers optimal results for wall cladding. This blend revealed low water absorption (0.84%), high compressive strength (17 MPa), and high impact strength (1.494 Joules). The hot-mixing process was conducted under a controlled temperature of 250 °C. Additionally, PET plastic waste has revealed a flash point of 355 °C and a fire point of 360 °C. XRF analysis showed that the composite cladding was primarily composed of 84.8% SiO<sub>2</sub> from river sand, indicated a loss on ignition value of 1.4%, and a low concentration of impurities such as Al<sub>2</sub>O<sub>3</sub>, Fe<sub>2</sub>O<sub>3</sub>, CaO, MgO, SO<sub>3</sub>, Na<sub>2</sub>O, K<sub>2</sub>O, P<sub>2</sub>O<sub>5</sub>, TiO<sub>2</sub>, and Cr<sub>2</sub>O<sub>3</sub>. These findings confirm the sand's suitability for wall cladding and other construction purposes. Despite the potential and increasing popularity of plastic waste as composite materials in the wider construction industry due to their outstanding properties, their specific inclusion for wall cladding applications remains significantly limited [18]. Critically, existing research often does not adequately address the unique performance requirements of wall cladding or fully explore the benefits of integrated PET plastic, sand, and recycled steel fiber reinforcement for this particular use. Therefore, this research presents a novel assessment into the strategic addition of recycled steel fibers to PET-based composites, aiming to enhance their mechanical properties and durability, particularly for demanding wall cladding applications [19, 20].

Recycled fibers, particularly those derived from waste vehicle tires, provide significant benefits when integrated into composite materials. These fibers are famous for improving compressive and impact strength and enhancing fire resistance [19, 21]. In lightweight concrete and composites, fibers are mainly integrated to minimize density and increase thermal insulation properties [22]. Their application can significantly reduce crack width under load, enhancing mechanical properties and durability in composite materials [23]. Various steel fiber contents, 0%, 0.5%, 1%, 1.5%, and 2% can be utilized to reinforce polymer composites [24, 25]. Tire-recycled steel fiber (0–3%), utilized in the mechanical performance evaluation of reinforced concrete [26, 27]. The mechanical resistance of ultra-high-performance geopolymer concrete and other composites is critically enhanced by adding steel fibers. In this regard, a 1% addition of steel fibers can significantly improve the impact resistance, flexural toughness, and hardness performance of ultra-high performance geopolymer concretes [28]. Several studies have explored optimal fiber content: [29] suggests that a 1% fiber content is optimal for improving the mechanical properties

of composites, while [30] established that a 1% steel fiber content typically enhances the mechanical strength of recycled concrete. A review by [31] On concrete reinforced with recycled steel fibers from waste tires, an optimal amount of 3% by mass has shown an impact on mechanical strength. However, it is important to note that while fibers increase strength, a higher volumetric content of fibers can create pathways for water ingress into the composite, especially if their orientation is unfavorable [32]. Whereas, a lower volumetric content can offer reduced porosity [32]. Moreover, short steel fibers have been exhibited to exceptional hardness and toughness in concrete and other composites when compared to longer fibers at equivalent dosages [33]. Incorporating fibers in composites is a mechanism that controls the crack bridging action during macro and micro fracture of the matrix. Steel fibers increase the energy absorption capacity of the composite by resisting the spread of microcracks, hence increasing the toughness of the composites [27]. Fiber bridging occurs when a crack moves from one matrix interface to another, leaving behind an unbroken fiber for crack deflection [34]. Previous studies have extensively investigated the use of steel fibers in composite materials. For instance, [35] investigated the integration of stainless steel wire into cladding layers. Similarly, studies by [36] and [37] revealed that adding steel fibers typically improved the mechanical properties of titanium/aluminium composite plates and steel-aluminium composite panels, respectively. [37] also suggested that a larger fiber diameter could contribute to increased tensile resistance.

Plastic composite claddings also have numerous disadvantages despite their advantages. These include a high initial cost that must be carefully considered against long-term benefits [38]. They can also suffer from fading in lower-quality or poorly developed products [39] and are prone to expansion and contraction with temperature variations, necessitating precise installation [40]. A significant

challenge also presents in their end-of-life recyclability, as their multi-material composition contributes to effective separation and reprocessing being difficult and often costly, potentially resulting to landfill disposal [41].

Given these challenges and the potential of recycled materials, this study particularly examined the suitability of integrating recycled tire steel fibers into PET-based wall cladding materials. By combining the properties of recycled PET and recycled steel fibers, the composite cladding materials with enhanced mechanical properties were produced. This research aims to contribute to the production of sustainable and high-performance wall cladding material for buildings in Tanzania. The successful implementation of the products is intended to result in a reduced environmental impact caused by plastic waste and offer creative solutions for the construction industry.

## Materials and methods

### Materials

The key materials used in this study were waste PET plastics, natural river sand, and recycled tire steel fibers. PET waste bottles were obtained from the Nsalaga dumpsite in Mbeya, Tanzania. Figure 1 displays photographs of shredded PET plastic, river sand, and recycled tire steel fibers. After thorough washing and drying, they were shredded into approximately 15-cm-long by 5-cm-wide pieces to prepare them for further processing and use in the composite material development process. The sand used in this study was collected from the Kamawe River in Rukwa Region, Tanzania, and then transported to the laboratory for further processing and use to make the composite PET wall cladding materials. Recycled steel fibers used in this study were obtained from waste vehicle tires located in Soweto vehicle



**Fig. 1** Shows the shredded PET plastic (A), sand (B), and recycled steel fibers (C)

service areas (garages) in Mbeya, Tanzania. The waste tires were incinerated for 2 to 3 h to ensure steel fibers were clean and free from contaminants. This process was followed by a cooling period before storing and utilizing it for making composite PET cladding.

### Characterization of raw materials

PET waste plastic bottles, river sand, and recycled steel fibers were subjected to different tests to determine their physical and chemical properties. These tests included density, melting temperature, flash and fire points for PET waste plastic bottles, particle size distribution, chemical composition, and density for sand [17]. Also, density, average length, and diameter were determined for recycled steel fibers. The recycled steel fibers employed in this study were sourced from waste tires, where the rubber component is recovered through an incineration process to uncover the embedded steel. When this incineration is conducted commercially, it typically incorporates advanced emissions control mechanisms to mitigate potential environmental impacts.

The sample of river sand was dried in an oven at 105 °C for 24 h to extract excess moisture. The PET waste plastic bottles were shredded into nearly 15 cm by 5 cm samples, then air-dried for 24 h. The 0.3 mm diameter recycled steel fibers were cut into approximately 1.5 cm pieces. A digital electric balance was used to measure the weight of each sample material. A known volume of water was recorded using measuring cylinders. The volume of sand, PET plastic, and steel fiber samples was determined by immersing the sample in the water cylinder and subtracting the original water volume. The densities of PET waste plastics, sand, and recycled steel fibers were determined as per procedures stipulated in [42]. The density of each sample material was computed using Eq. 1 [36].

$$\text{Density } (\rho_s) = \frac{M}{V_2 - V_1} \quad (1)$$

where  $M$ —is mass of sample,  $V_1$ —is volume of sample of water in cylinder,  $V_2$ —is volume of water and sample materials in cylinder.

A relative difference between the combined density of the individual materials and the density of the hot-mixed cladding specimens would indicate that chemical reactions occurred during the blending process [44].

PET waste plastic samples indicated a melting temperature of 240–255 °C. This temperature range was determined by the hot plate method after three iterations for accurate thermometer readings. Similarly, using the Cleaveland open cup apparatus and the procedures stipulated in MoW, 2000 [42], the shredded PET plastic samples used in this study

had a flash point of 355 °C and a fire point of 360 °C [17]. These temperatures were examined before hot mixing in order to prevent material ignition. PET plastics may burn to ashes if the mixing temperature exceeds the flash point, rendering them ineffective as a binder for sand and recycled steel fibers.

The oxide compositions of the river sand and PET waste plastics were determined by using X-ray fluorescence (XRF) techniques. The sand samples were ground to a 3656 cm<sup>2</sup>/g particle size using a ball mill, and the PET waste plastics were incinerated to ash. The distribution of each element was quantified and presented as a percentage by weight. Table 1 indicates the oxide compositions of the sand and PET plastic ash used in this study. Verifying the oxide composition of components, particularly sand, is fundamental because the chemical composition of components influences other component properties, including heat resistance and strength. Sand materials with a high silica content of over 80% can withstand temperatures exceeding 600 °C [45, 46].

A sieve analysis of the river sand sample was conducted following the procedures outlined in [41]. A wet sieving test was performed, and the percentage of sand particles passing through each standard sieve size was measured. The river sand was passed through a 600 μm sieve, which is the recommended maximum sand size for blending with PET waste plastics and steel fibers to produce cladding and tile specimens [45]. Figure 2 shows the particle size distribution curves of sand that passed through the 600 μm sieve.

### Composite cladding materials

Fifty percent (50%) by weight of the river sand (passing through a 600 μm sieve) was primarily blended with recycled steel fibers, followed by the incorporation of 50% by weight of shredded PET waste plastics. The 1:1 sand to PET ratio was selected due to previously determined best performance in compressive strength [17]. Recycled steel fibers were included in varying percentages of 0.5%, 1%, 1.5%, 2%, 2.5%, 3%, 3.5%, 4%, 4.5% and 5% by weight during the production of specimens. The selected increment step size was designed to ensure sufficient data points, to accurately observe and analyze trends in mechanical performance across the specified range. Sand, recycled steel fibers, and PET waste plastics were hot mixed under a controlled temperature of 250 °C. The mixture of sand and recycled steel fibers was first heated in a 50 cm × 50 cm steel mold at a temperature of 240 °C for 6 min. Then, shredded PET waste plastics were added and continuously stirred until fully melted and homogeneously mixed with sand and recycled steel fibers. This pre-heating of sand and steel fibers at 240 °C was essential for two reasons: first, to ensure the

**Table 1** Elemental composition of sand and PET plastic ash, as done by the XRF machine

Oxides (%)	SiO <sub>2</sub>	Al <sub>2</sub> O <sub>3</sub>	Fe <sub>2</sub> O <sub>3</sub>	CaO	MgO	SO <sub>3</sub>	Na <sub>2</sub> O	K <sub>2</sub> O	P <sub>2</sub> O <sub>5</sub>	TiO <sub>2</sub>	Cr <sub>2</sub> O <sub>3</sub>	LOI
River sand	84.8	6.35	6.06	0.62	0.27	0.01	0.24	1.11	0.05	0.52	0.03	1.4
PET	62.11	5.95	6.02	1.02	0.19	0.23	0.2	1.03	0.06	0.84	0.02	23.25

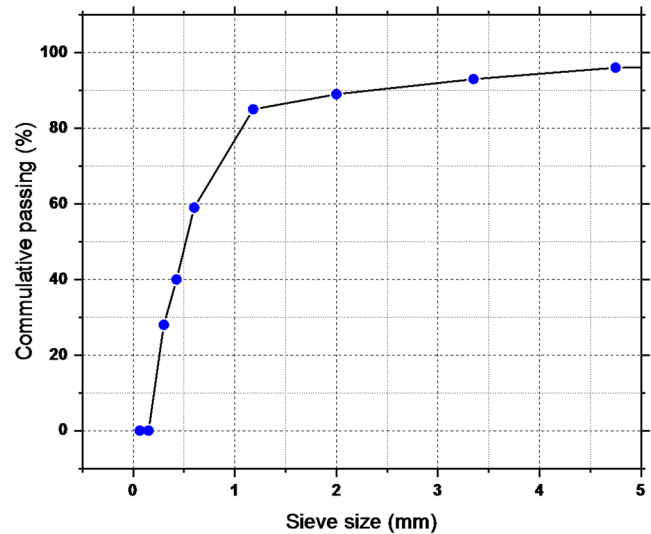


**Fig. 2** Particle size distribution curve of graded sand passed through 600 µm sieve

sand and steel fibers were dry, which prevents steam generation and potential void formation in the final composite cladding. Second, it was to bring sand and steel fibers to a temperature very close to the PET’s melting point (240–255 °C), enhancing the wetting efficiency of the sand and steel fibers by the molten PET. This approach minimized thermal shock to the melting PET, promoting a uniform distribution of all components throughout the matrix. The melted mixture was poured into an oiled 24.4 cm × 12.2 cm by 2 cm mold, compressed, and cured at room temperature to produce a composite wall cladding panel specimen. This technique was repeated for each recycled steel fiber percentage while maintaining a constant PET plastic waste and sand ratio. Firing processes are carried out using a locally fabricated steel pot furnace fueled by waste wood dust and rice husks. Mixing temperatures were monitored using a 1500 °C digital thermometer. Figure 3 displays hot-mixed cladding specimens. Laboratory evaluation was done to estimate water absorptions, densities, compressive strengths, and impact strength properties of hot-mixed composite cladding specimens.

The densities of the cladding composite materials were evaluated according to the procedures outlined in [42]. The specimens were weighed using a digital electronic balance, and their weights were recorded. A graduated plastic bucket was filled with a known volume of water. The specimens were then immersed in the water, and the water levels were recorded. The densities of the specimens were computed using Eq. 1. Table 2 displays the densities of the hot mixed cladding specimens for each PET-sand-steel fibers mixture. Finding out the density of the cladding specimens is important for understanding their weight, specifically for transportation and handling purposes during installation on walls.

**Fig. 3** Cladding composite materials with different steel fibers contents

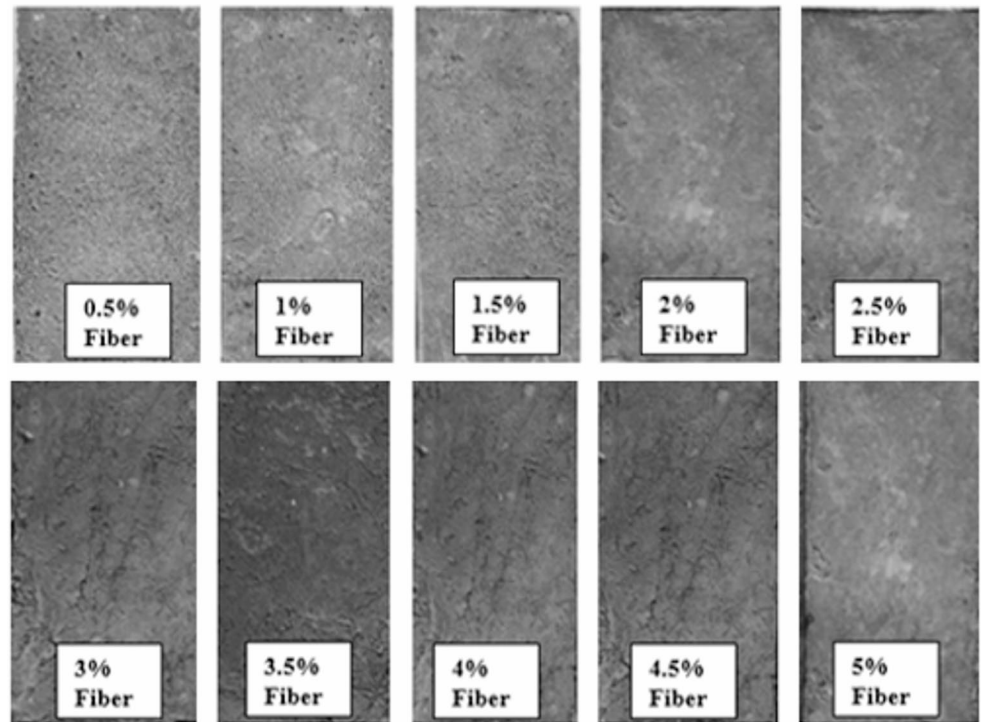


**Table 2** Physical properties of the composite Cladding material

Composite materials			Average water absorption (%)	Average density of specimens (g/cm <sup>3</sup> )
PET (%)	Sand (%)	Steel fibers (%)		
50	50	0	0.84	1.622
		0.5	0.8	1.644
		1	0.71	1.815
		1.5	0.68	2.009
		2	0.65	2.205
		2.5	1.8	2.469
		3	2.4	2.687
		3.5	3.1	2.708
		4	3.6	2.74
		4.5	4.1	2.796
		5	4.7	2.852

However, high weights of cladding can result in increased self-weights of the building, causing a risk of cladding panel collapse, especially at higher heights or floor levels.

The water absorption of the cladding specimens were determined according to the procedures outlined in [42]. The digital electric balance was used to weigh cladding composite specimens. The specimens were then immersed in clean water inside plastic buckets for 24 h, removed, wiped with a cotton cloth to remove surface water, and reweighed. The percentage water absorption for each specimen was computed using Eq. 2 [42, 47].

Evaluation of water absorption is important for assessing the amount of water that is absorbed by cladding specimens

and, consequently, the wall, particularly during rainfall, and to control dampness within buildings.

$$\text{Water absorption (\%)} = \frac{(M_2 - M_1)}{M_1} \times 100 \quad (2)$$

where  $M_2$ —is the mass of the water surface dry specimen after immersion in water, and  $M_1$ —is the mass of the specimen before immersion in water.

The compressive strength of the composite cladding specimens was estimated using a rebound hammer. A total of nine rebound hardness readings were measured for each specimen: three at each edge and three at the center. The average rebound hardness value was computed for each sample. These average rebound hammer readings were then modified to compressive strengths using Eq. 3 [48].

$$\text{CS (Mpa)} = 0.788R^{1.03} \quad (3)$$

where CS—is compressive strength of specimen (MPa), R—is rebound hammer reading.

Table 3 displays the rebound hammer readings of every composite cladding specimen. Evaluating the compressive strength of composite cladding specimens is fundamental to assessing their breakage resistance during transportation and handling during installation.

The impact strength of the composite cladding specimens was evaluated using a drop-weight impact test. A 338.8 g steel ball with a 4.54 cm diameter was dropped on top of

**Table 3** Rebound hammer readings on composite cladding material

Sample Specimen	Rebound hammer readings						Average readings	Compressive strength (MPa)	
	Steel fiber	Left		Center		Right			
50PET50Sand	0.0%	20	16	20	26	18	26	20.1	17.33
	0.5%	20	20	20	20	20	23	21.22	18.32
	1.0%	23	21	21	26	26	23	23.44	20.3
	1.5%	28	26	24	24	24	23	24.66	21.39
	2.0%	26	26	26	25	28	25	25.88	22.48
	2.5%	25	26	24	27	26	27	26	22.59
	3.0%	27	25	26	25	26	28	26.22	22.79
	3.5%	22	32	26	28	24	30	25.77	22.39
	4.0%	24	24	25	22	24	22	23.22	21.31
	4.5%	22	24	25	22	21	23	23.88	20.7
	5.0%	23	24	23	26	22	22	23.44	20.3

specimens from heights of 30 cm, 60 cm, and 90 cm. The ball was guided by a 100 cm steel bar during the test. Six points (two at each edge and two at the center) were examined for fracture for each specimen. Depth of penetration and cracks length on the surface of the specimen were visually observed and measured using a ruler. The impact energy (IE) was computed for each drop height using Eq. 4 [20].

$$IE \text{ (Joules)} = M_{sb} \times G \times H \tag{4}$$

where IE—is impact energy (Joules),  $M_{sb}$ —is mass of steel ball (kg),  $G$ —is acceleration due to gravity ( $10 \text{ m/s}^2$ ),  $H$ —is drop height (m).  $H (H_{initial} - H_{rebound})$ .

The rebound height ( $H_{rebound}$ ) was measured using a ruler at three points (center and each edge) to determine the absorbed energy ( $E_{absorbed}$ ). The standard deviation of absorbed energy was calculated for reinforced steel fiber composite specimens for 1–5% fiber content using Eq. 5. The observed damage and calculated absorbed energy were utilized to assess the impact strength of the composite cladding specimens. This evaluation is critical for understanding the ability of cladding to withstand shocks and prevent from complete collapse of the installed composite cladding panels. Figure 4 shows photographs of the experimental setup for the compressive strength test (using the rebound hammer method), the impact strength test (using a dropping steel ball), and the water absorption test (using a plastic soaking container).

All observed data, including average water absorption, density, compressive strength, and impact strength, were subjected to further statistical analysis to calculate their standard deviations. This statistical measure quantified the spread of the data for each property. A higher standard deviation demonstrates greater spread of data points from the average, showing more variability; a lower standard deviation indicates data points concentrated more closely around the average, indicating greater uniformity within the measured property. The standard deviation and confidence interval for the reinforced steel fiber composite cladding material were calculated using Eqs. 5 and 6 [26, 49–51].

$$S = \sqrt{\frac{\sum_{i=1}^n (Xi - X)^2}{n - 1}} \tag{5}$$

where  $S$ =Sample standard deviation,  $Xi$ =individual data point,  $X$ =sample mean,  $n$ =number of observations/data points in the sample

$$C = X \pm \frac{t\alpha}{2, df} \left( \frac{s}{\sqrt{n}} \right) \tag{6}$$



**Fig. 4** Photographs of Rebound hammer test (A), Ball impact strength test (B), and Water absorption test (C)

where  $C$  = Confidence Interval,  $X$  = Sample mean or Point Estimate,  $t_{\alpha/2, df}$  = Critical t-value from the t-distribution,  $df$  = degree of freedom =  $(n - 1)$ ,  $s$  = sample standard deviation,  $n$  = sample size.

### Thin section of PET cladding for petrographic analysis

Petrographic analysis was conducted on composite material specimens containing 1%, 2%, 3%, and 4% steel fibers to examine their microstructure. Samples were sectioned into 4–5 mm chips by using a diamond-impregnated saw. These chips were labelled, dried, and mounted onto glass slides (46 mm × 27 mm × 1 mm) to produce standard petrographic thin sections. Petrographic analysis of thin sections was conducted at the Mineralogy, Petrology, and Gemology Services laboratory located in Dar es Salaam.

The thin sections were analyzed by using a Leica DM 750P polarized light microscope. Images were captured with a Leica camera at 50× magnification, with some additional images taken at 100× magnification to highlight specific features. Images were taken at 1600 × 1200 pixels resolution, with a field of view of 7 mm. The microstructure of the composite PET cladding samples was examined to characterize void content, fiber distribution, and fiber orientation.

## Results and discussion

### Characterization of sand, PET waste plastics, and recycled steel fibers

Laboratory characterization tests on the PET plastics obtained a density of 1.305 g/cm<sup>3</sup>, a melting temperature range of 240–255 °C, a flash point of 355 °C, and a fire point of 360 °C. Given that PET is a semi-crystalline polymer,

which means it has both amorphous and crystalline regions, its melting temperature is generally reported within the range of 245–260 °C, with some literature citing ranges such as 240–260 °C [52–54]. A hot plate method allows for visual observation of this solid-to-liquid transition, and the observed 240–255 °C range falls within or very close to the reported melting range for PET. Therefore, it is most appropriate to describe this observed range as the melting temperature of the PET waste plastic sample. Furthermore, the recycled steel fibers had a density of 7.79 g/cm<sup>3</sup>, a diameter of 0.3 mm, and an average length of 1.5 cm.

The sand used in this study possessed a 2.59 g/cm<sup>3</sup> density, a mean size (D50) of approximately 0.33 mm, and a uniformity coefficient ( $C_u$ ) of about 2.44. The obtained  $C_u$  value indicates a uniformly graded sand. Although this coefficient results in lower density and higher permeability, the inclusion of recycled PET plastic and steel fibers in the composite cladding alters the sand properties.

XRF analysis (Table 1) revealed that the sand is composed of SiO<sub>2</sub> at 84.8% content. Major oxide components, including Al<sub>2</sub>O<sub>3</sub>, Fe<sub>2</sub>O<sub>3</sub>, CaO, MgO, SO<sub>3</sub>, Na<sub>2</sub>O, K<sub>2</sub>O, P<sub>2</sub>O<sub>5</sub>, TiO<sub>2</sub>, and Cr<sub>2</sub>O<sub>3</sub>, were also present. The loss on ignition value of 1.4% is well below the 5% limit for construction purposes, indicating minimal organic or carbonate content. While Iron (Fe<sub>2</sub>O<sub>3</sub>) was demonstrated at 6.06%, a typical impurity that may alter sand properties depending on its level, its concentration level in the sand did not compromise the sand's suitability for wall composite cladding materials. Other impurities such as Al<sub>2</sub>O<sub>3</sub> (6.35%), MgO (0.27%), and TiO<sub>2</sub> (0.52%) are present at low levels (each below 10% of their total weight). Trace elements such as Zr, Sr, Ba, and S were also identified in low levels (0.08%, 0.20%, 0.14%, and 0.06%, respectively) [16]. XRF analysis confirmed that the high SiO<sub>2</sub> content and low concentration of impurities, as confirmed by XRF analysis, collectively verify the sand's

suitability for composite wall cladding materials and construction purposes.

### Density of cladding composite

As shown in Table 2, the density of the composite cladding increased with the addition of recycled steel fibers. The sample with 0% steel fiber content had demonstrated the lowest average density at 1.622 g/cm<sup>3</sup>, while the 5% steel fiber sample had the highest density at 2.852 g/cm<sup>3</sup>. This trend aligns with the increased mass established by the higher proportion of steel fibers, which have a higher specific gravity than the base composite material [32]. Figure 5 displays the density curve of steel fiber-reinforced composite cladding.

The water absorption characteristics of the PET composite cladding, containing different proportions of recycled

steel fibers, were studied under laboratory conditions. Figure 6 shows the correlation between steel fiber content and water absorption. Generally, the water absorption of the composite ranged from 0.65 to 4.70%. Specifically, the specimens with 0–2% steel fibers indicated a reduction in water absorption from 0.842 to 0.65%. This reduction is likely due to decreased void space as steel fiber content increased. However, further increases in steel fiber content, from 2.5 to 5%, led to a rise in water absorption, from 1.8 to 4.7%. This increase is likely due to the formulation of more void space with a higher proportion of steel fibers [32]. When compared to the typical water absorption classifications for ceramic tiles, the specimen with 0–3% fiber content exhibited properties consistent with vitreous materials, while those with 3.5–5% fiber content aligned with semi-vitreous materials as per ASTM C373 [55]. This trend can be related to several factors, such as the initial addition

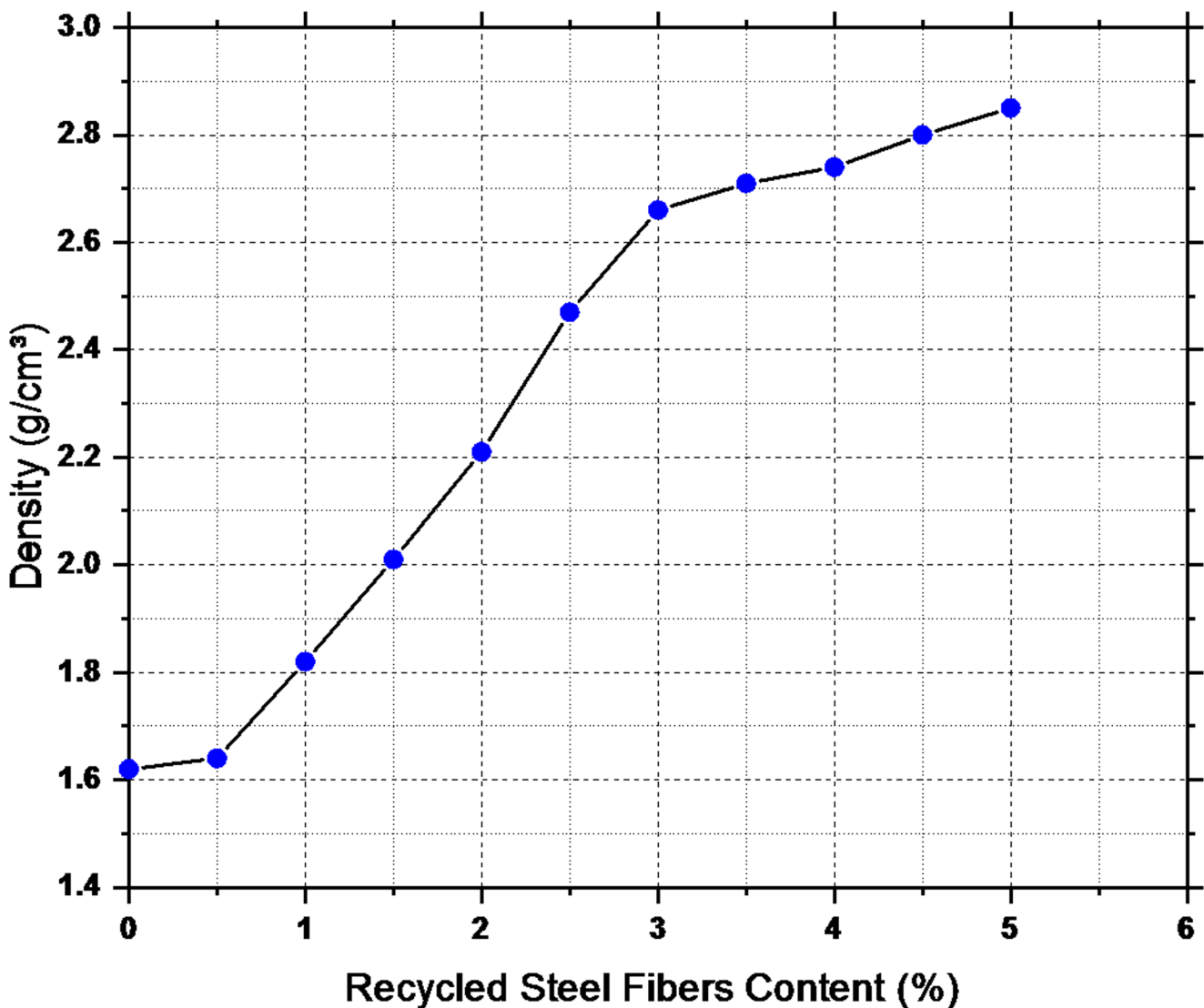
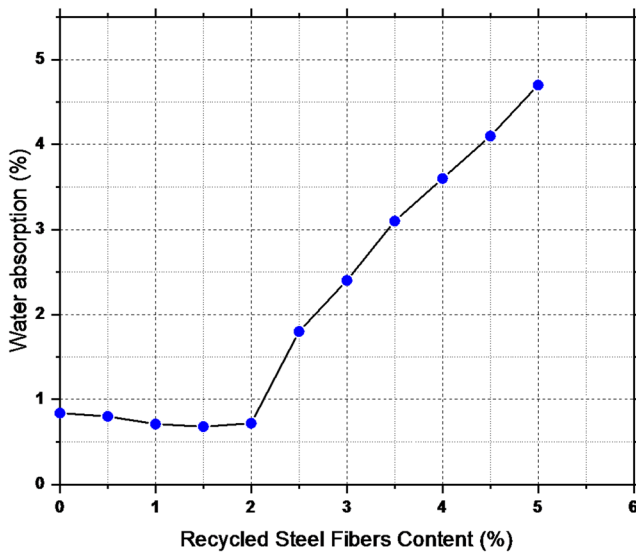


Fig. 5 Density curve of Reinforced PET composite cladding materials



**Fig. 6** Water absorption curve of Reinforced PET composite cladding materials

of steel fibers may have reduced porosity and improved the material's resistance to water absorption, and greater concentration of fibers can create routes for water to enter the composite, particularly if their orientation is unfavorable [20, 32].

Based on the observations, composite material specimens with a PET plastic to sand ratio of 1:1, and the addition of 1%, 1.5%, and 2% recycled steel fibers proved exceptionally low water absorption rates, making it highly suitable for wall cladding applications. While other percentages (0.5%, 2.5%, and 3%) also demonstrated water absorption rates within the recommended range of 0.5–3% [8]. High resistance to moisture infiltration is vital to avoid structural degradation, securing the lifespan and durability of external wall claddings.

The variability and reliability of average water absorption and density measurements for composite specimens with varying steel fiber contents were analyzed using standard deviations and 95% confidence intervals. This analysis addressed distinct behavioral trends for each property, providing crucial insights for the material's application as cladding. Table 4 demonstrates these results for the composite materials' water absorption and density.

The average water absorption showed a high standard deviation (1.533), indicating considerable data dispersion across composite formulations. This suggests that the amount of steel fiber greatly influences water absorption, resulting in a wide range of values. The 95% confidence interval of [1.095, 3.156] emphasizes this variability, covering an approximate range of 2.06%. This significant fluctuation in water absorption is an important factor for cladding

**Table 4** Statistical analysis for the average water absorption and density of reinforced steel fiber composite cladding materials

Property	Standard deviation	95% confidence interval
Average water absorption of the specimens (%)	1.533	1.095, 3.156
Average density of the specimens (g/cm <sup>3</sup> )	0.480	2.000, 2.645

materials, as it directly impacts durability and thermal insulation.

On the other hand, the average density showed a lower standard deviation (0.480), indicating greater consistency in measurements despite the overall increase in density with higher fiber content. The 95% confidence interval of [2.000, 2.645] is narrower, about 0.645 g/cm<sup>3</sup>, emphasizing this trend of more predictable density values. Understanding these different variabilities in water absorption and density is crucial for quality control, performance prediction, and optimizing the design of reinforced steel fiber composite cladding materials. Further analysis could examine the specific trends of water absorption and density relative to each steel fiber percentage to identify optimal ranges or thresholds.

### Compressive strength of reinforced composite PET cladding materials

Figure 7 indicates a positive correlation between compressive strength (N/mm<sup>2</sup>) and steel fiber content (%) in the composite PET specimens. The addition of steel fiber contents at 0%, 0.5%, 1%, 1.5%, 2%, 2.5%, and 3%, resulted in increased compressive strengths 17.33 N/mm<sup>2</sup>, 18.32 N/mm<sup>2</sup>, 20.30 N/mm<sup>2</sup>, 21.39 N/mm<sup>2</sup>, 22.48 N/mm<sup>2</sup>, 22.59 N/mm<sup>2</sup> and 22.79 N/mm<sup>2</sup> respectively. Similarly, further increases in fiber contents at 3.5%, 4%, 4.5%, and 5% resulted in a decreased trend of compressive strength values of 22.39 N/mm<sup>2</sup>, 21.31 N/mm<sup>2</sup>, 20.70 N/mm<sup>2</sup>, and 20.30 N/mm<sup>2</sup>, respectively. This downfall is likely attributed to factors such as increased void formation, insufficient wetting, and poor fiber distribution within the matrix [21].

The overall enhancement in compressive strength, especially with optimal fiber content, is linked to the reinforcement effect of the steel fibers. These fibers act as bridges, effectively transferring loads, resisting crack growth, improving toughness, and increasing the overall stiffness of the composite matrix [20]. However, excessive fiber content can negatively affect mechanical properties due to insufficient wetting, increased voids, and poor fiber distribution [21]. The critical volume was found to be between 2% and 3.5%. Specimens within this range demonstrated breaking

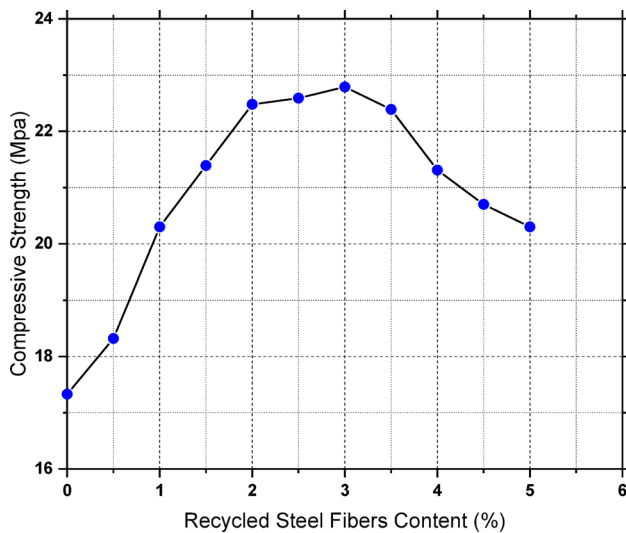


**Fig. 7** Compressive strength curve of Reinforced PET composite cladding materials

**Table 5** Statistical analysis for rebound hammer readings of reinforced steel fiber composite materials

Sample	Steel fiber	Mean rebound hammer reading	Standard deviation	95% Confidence interval
50PET50Sand	0.0%	20.10	3.62	17.20, 23.03
	0.5%	21.22	1.86	19.74, 22.70
	1.0%	23.44	1.94	21.89, 24.99
	1.5%	24.66	1.80	23.28, 26.05
	2.0%	25.88	1.17	24.97, 26.81
	2.5%	26.00	1.22	25.04, 26.96
	3.0%	26.22	0.97	25.46, 26.99
	3.5%	25.77	3.49	22.98, 28.57
	4.0%	23.22	1.09	22.36, 24.08
	4.5%	23.88	2.20	22.14, 25.63
	5.0%	23.44	1.42	22.31, 24.58

strength and modulus of rupture properties comparable to those of ceramic tiles, as per ASTM C1505 [56].

The statistical analysis of steel fiber reinforced composite materials was achieved by focusing on rebound hammer readings and compressive strength. This analysis highlighted the significance of standard deviation as a measure of data dispersion and confidence intervals for estimating the true sample mean. Table 5 shows the standard deviation and confidence intervals of rebound hammer readings of reinforced steel fiber composite cladding material.

The rebound hammer readings revealed that material consistency varies significantly with steel fiber percentage. The 3.0% fiber content exhibited the most uniform readings (lowest standard deviation of 0.972 and narrowest confidence interval), indicating optimal consistency. On the other hand, the 0.0% and 3.5% fiber samples demonstrated the highest variability (standard deviations of 3.621 and 3.492,

respectively), pointing to less uniform surface characteristics. Finally, the collective compressive strength had a standard deviation of 1.865 MPa and a 95% confidence interval of [19.710, 22.217] MPa, indicating a reasonably predictable average strength across the tested range of fiber content. Briefly, the statistical analysis confirms that the steel fiber content significantly influences the uniformity and performance of the composite, with particular percentages yielding more uniform and predictable properties crucial for quality assurance and design enhancement of cladding materials.

### Impact strength of PET composite cladding materials

The material’s impact resistance was investigated through six controlled steel ball drops on each specimen at varying heights. Initial findings indicated no visible damage was detected across all specimens for 30 cm and 60 cm drop heights. This reveals a uniform baseline resistance to lower energy impacts for all material compositions tested.

However, a significant difference in impact performance was observed at higher energy levels. Specimens without significant fiber reinforcement, particularly those with 0% and 0.5% recycled tire steel fibers, cracked upon impact from a height of 90 cm. Conversely, the samples possessing 1–5% recycled steel fibers demonstrated superior resilience, revealing no cracking at 90 cm drop height. This preliminary finding addresses the key role of steel fiber inclusion in enhancing the material’s resistance to higher energy impacts.

The reinforced composite cladding specimens with 1–5% fiber content were further investigated to quantify improved performance. Table 6 presents the detailed results of mean energy absorption, standard deviation, and sample counts of reinforced composite cladding materials:

As observed in Table 6, the mean energy absorption for the 1–5% fiber contents exhibits a slight increasing trend, progressing from 2.913 Joules at 1% fiber content to 3.037 Joules at 5% fiber content. This indicates that higher volumetric content of steel fibers consistently leads to an enhanced capacity for energy absorption under impact. This revealed enhancement in impact strength is directly related to the well-established reinforcement effect of the steel fibers within the composite matrix, which effectively act as bridges across essential crack paths, thereby transferring loads, resisting crack propagation, typically improving the material’s toughness, and enhancing stiffness [20]. The fiber’s ability to distribute stress and mitigate brittle fracture is crucial to its role in energy absorption under impact loading.

**Table 6** Energy absorption of reinforced composite cladding material

Sample	Fiber content (%)	Mean energy absorption (Joules)	Standard deviation (Joules)	Sample count (n)
50PET50SAND	1%	2.913	0.029	3
	2%	2.986	0.010	3
	3%	3.010	0.008	3
	4%	3.010	0.022	3
	5%	3.037	0.012	3

Furthermore, the standard deviation values across each fiber content group (0.029, 0.010, 0.008, 0.022, and 0.012 Joules) are uniformly low. This indicates a relatively uniform and favorable degree of variability within each measured specimen, underscoring the robustness of the experimental methodology. Such uniformity across groups also implies a stable and uniform mechanical behavior from the material at varying fiber concentrations.

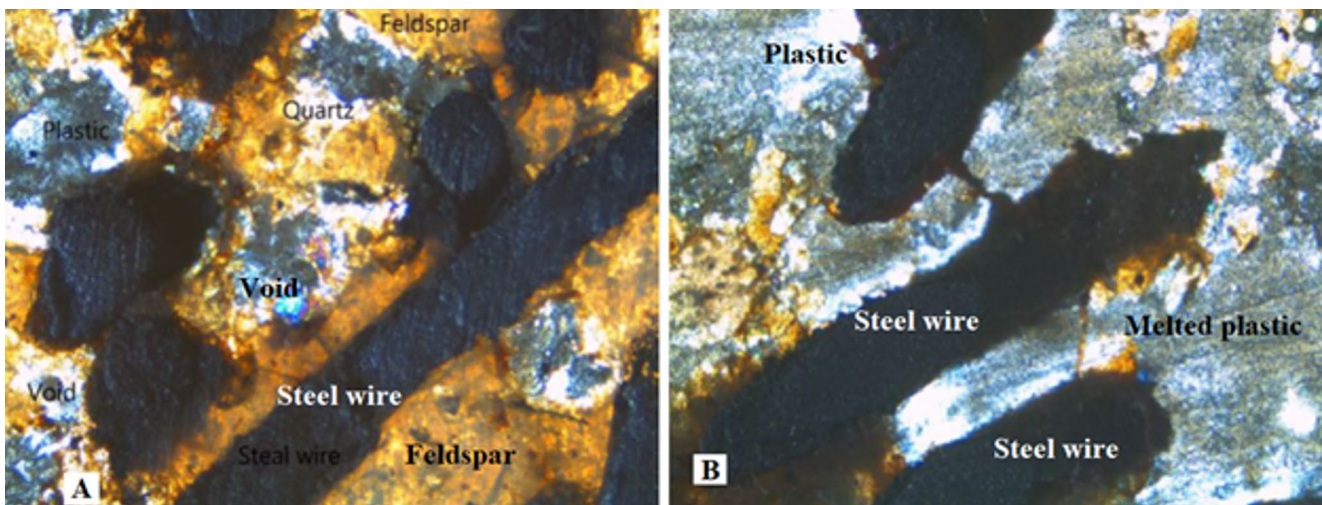
For all fiber contents (1–5%) investigated, the overall mean absorption energy was determined to be 2.991 Joules, with a corresponding average standard deviation of 0.016 Joules. These comprehensive statistical metrics (Mean energy absorption, standard deviation, and sample count for each fiber content) offers a complete and reliable interpretation of the experimental data, validating the observed trends and uniformity of energy absorption characteristics across the varying fiber percentages.

On the basis on these findings, it is evident that the incorporation of steel fibers significantly improves the impact resistance of the composite. This observation further indicates the significance of achieving an optimal balance among the constituent materials (PET plastic, sand and recycled steel fibers) to optimize impact resistance for specific cladding applications [21].

## Petrographic analysis of PET composite cladding material

Petrographic analysis was conducted on composite material specimens containing 1%, 2%, 3%, and 4% steel fibers to characterize their microstructure. Figure 8 reveals a petrographic photograph of composite cladding with 1% recycled steel fibers. The analysis has indicated that the PET composite specimens are composed of very fine, round to sub-round silt to sand-sized quartz crystals. Opaque isotropic Iron oxide (hematite) intergrown with quartz and very few weathered plagioclase feldspar grains, as well as a plastic matrix. However, a few flakes of mica minerals, mainly biotite and muscovite, were also observed in the microscope. Opaque black long stainless-steel wires, which were observed to be distributed randomly within the specimens. Sectioned samples displayed numerous angular to elongated voids, ranging in size from 2 to 5 mm, likely resulting from plastic material flow during production. Observations showed that some voids were filled with plastic and quartz sand. Steel fibers were observed to show both random (Figs. 8 and 9) and elongated distributions (Figs. 10 and 11) within the matrices.

The resulting images of the composite PET cladding material composed of 1% (Fig. 8) indicated that the voids within the specimens were predominantly round, and some elongated voids were also observed. Steel fibers were observed to be randomly distributed throughout the matrix, which increased the strength of the specimens, similar to observations in other studies [20, 21]. The molten PET plastics materials were used as binders to bind sand and steel fibers together; however, they were observed to fill the voids during the process of mixing, which eventually increased the strength of the composite PET cladding [57]. Figure 9

**Fig. 8** Composite Cladding material with 1% steel fibers

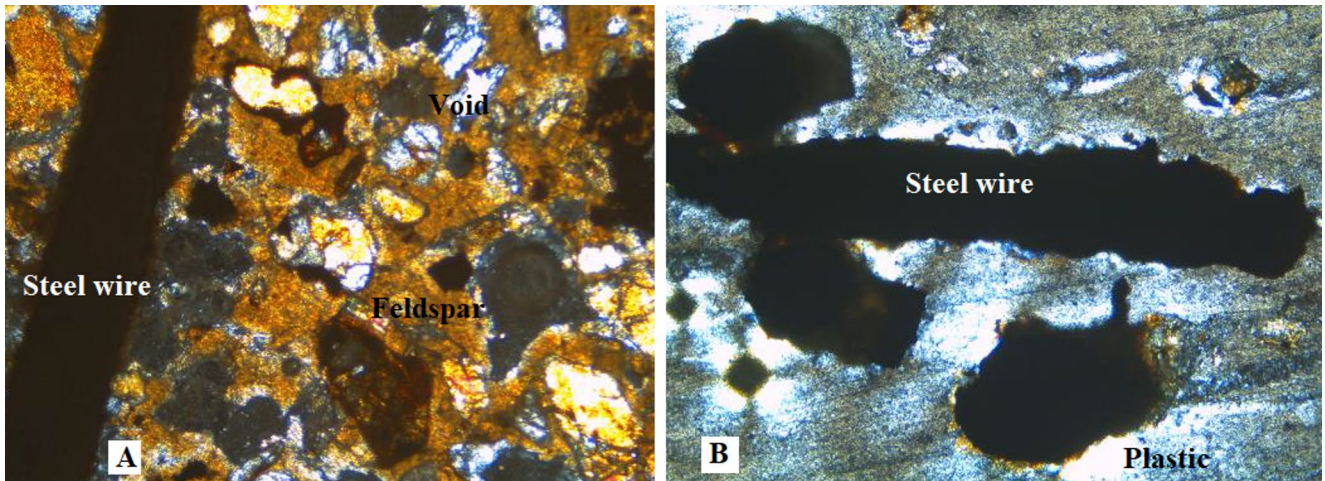


Fig. 9 Composite Cladding material with 2% steel fibers

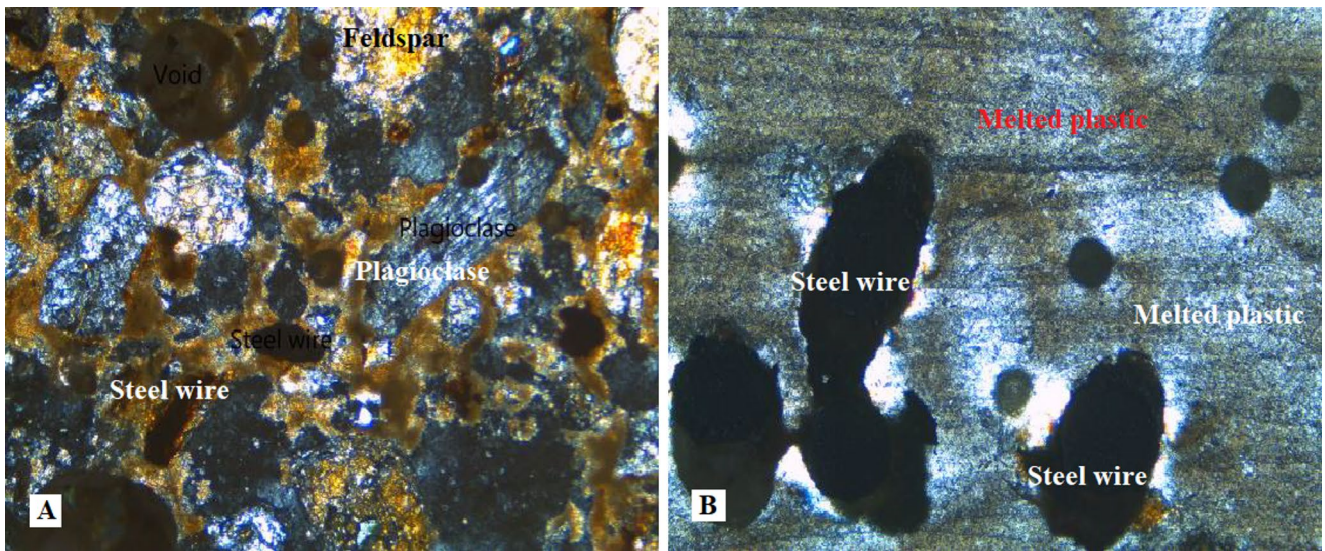


Fig. 10 Composite Cladding material with 3% steel fibers

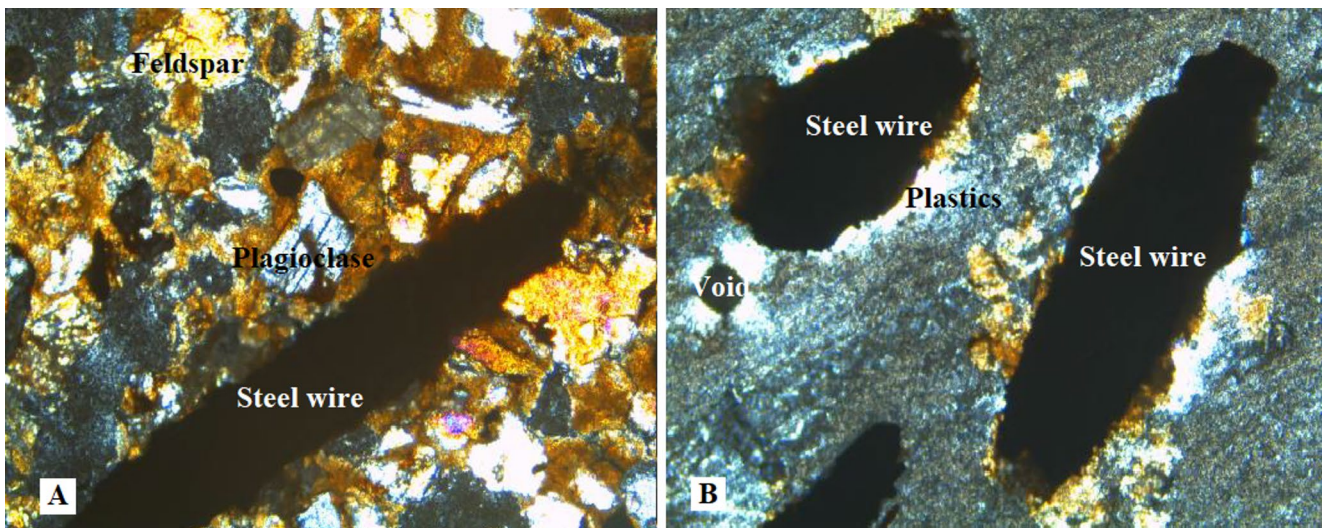


Fig. 11 Composite Cladding material with 4% steel fibers

displays a petrographic photograph of composite cladding with 2% recycled steel fibers.

The resulting images of composite PET cladding material composed of 2% steel fibers (Fig. 9) revealed that the voids within the composite were predominantly round, with some elongated voids also existing. Steel fibers were observed to be in a preferred distributed preferentially throughout the matrix, enhancing the strengthening of the specimen. Moreover, PET Plastic was recognized as the binder material, filling the voids and binding the quartz sand and steel fibers together [57]. Figure 10 reveals a petrographic photograph of composite cladding with 3% recycled steel fibers.

The resulting images of composite PET cladding material composed of 3% steel fibers (Fig. 10) revealed that the voids within the composite were predominantly round, with some elongated voids also existing. Steel fibers were observed to be in elongated orientation throughout the matrix, supporting the strengthening of the specimen. Furthermore, PET Plastic was recognized as the binder material, filling the round, angular, and sub-angular voids and adhering the quartz sand and steel fibers together [58]. Figure 11 reveals a petrographic photograph of composite cladding with 4% recycled steel fibers.

The resulting images of composite PET cladding material composed of 4% steel fibers (Fig. 11) showed that the voids within the composite were predominantly round, with some elongated voids also present. Steel fibers were observed to be in elongated orientation throughout the matrix, enhancing the strengthening of the specimen. Moreover, PET Plastic was recognized as the binder material, filling the round, angular, and sub-angular voids and binding the quartz sand and steel fibers together [58, 59].

Composite cladding development presents challenges, particularly concerning production energy consumption and the sourcing of recycled fibers. The developing process of composite cladding requires substantial energy, necessitating optimization and the possible incorporation of renewable energy sources to maintain environmental benefits. A reliable and high-quality supply of recycled PET plastic waste and steel fibers is also essential, requiring improved local collection infrastructure, strict quality control to manage variations in recycled material properties, and strong supply chain logistics. These efforts, combined with public participation in waste segregation, are essential to ensure the long-term viability and environmental integrity of this creative building material.

## Conclusion and recommendations

### Conclusion

This research successfully highlights the potential of transforming waste materials into a suitable and affordable wall cladding material. Experiments concentrated on composites made with sand (above 80% silica), recycled PET, and waste tire steel fibers at proportions of 0.5–5% by weight. The experiments exhibited that integrating steel fibers notably enhanced the mechanical performance. Compressive strength peaked at 22.8 MPa with a 3% steel fiber content, and a strength of 17.3 MPa was observed in specimens without fibers. This enhancement is related to the fiber's ability to bridge cracks, effectively distributing loads, and adding the material's toughness and stiffness. Moreover, impact testing revealed that specimens with 1–5% fiber content consistently absorbed impact energy without cracking, indicating excellent resistance, likely due to the fibers' effective distribution within the composite. Petrographic analysis confirmed this even distribution of fibers and a little porosity, with molten plastic covering pores and reinforcing the material's strength.

Therefore, 50% PET, 50% sand, and 2–3.5% recycled steel fibers are optimal for developing composite PET cladding materials. This combination yields a material with superior mechanical properties, including high impact and compressive strength, and low water absorption. These characteristics make it highly suitable for various wall cladding applications. Ultimately, this research offers a promising pathway to mitigate environmental concerns associated with plastic waste, diverting tons of waste from landfills. Similarly, it encourages sustainable building practices and provides a cost-effective cladding solution for construction projects. For instance, CTM Tanzania (a leading specialist retailer) reports that ceramic tiles in Tanzania cost approximately TZS 28,000 to 118,055.56 (USD 10.58 to 44.86) per square meter. This is significantly higher than TZS 10,000 (USD 3.78) per square meter for our locally created composite wall cladding. The composite wall cladding in this research is primarily intended for residential buildings. It suggested installation involves a battening system that ensures adequate ventilation and firm attachment. This process involving preparing the wall surface, seasoning the composite cladding panels to resist warping, installing battens to establish a ventilation gap behind the cladding, and using stainless steel screws driven into pre-drilled pilot hole for secure attachment. Further investigation is required especially regarding the scalability of production and long-term performance under environmental conditions.

## Recommendations

We recommend utilizing between 2 and 3.5% steel fiber content to optimize the mechanical properties of reinforced steel fiber composite wall cladding material.

Beyond this, Further research is recommended to evaluate the incorporation of various waste materials or additives, such as Rice husk ash (RHA), and ground granulated blast furnace slag (GGBS). This investigation aims to enhance the properties of plastic-based composites, essentially leading to additional improvements in mechanical performance, fire resistance, or other desired characteristics.

Furthermore, cost–benefit analyses should be conducted to evaluate the economic feasibility of large-scale production. This will help to investigate the potential cost savings and environmental benefits of integrating recycled PET plastic into construction projects.

Future research endeavors should also include quantitative methods for evaluating fiber distribution and porosity, utilizing relevant equipment and advanced analytical techniques. Additionally, further specific testing on long-term water resistance, moisture diffusion, and performance under humid conditions represents a crucial area for future investigation.

**Acknowledgements** The authors would like to express their sincere gratitude to the dedicated staff of TANROADS Rukwa, TANROADS Songwe and TARURA Mbeya for their administrative and logistic assistance throughout the duration of this research.

## Declarations

**Conflict of interest** The authors declare no conflict of interest.

**Research involving human participants and/or animals** This research did not involve human participants or animals

**Informed consent** This study utilized anonymized, publicly available data; informed consent was not applicable.

## References

- Evode N, Qamar SA, Bilal M, Barceló D, Iqbal HMN (2021) Plastic waste and its management strategies for environmental sustainability. *Case Stud Chem Environ Eng* 4:100142. <https://doi.org/10.1016/j.cscee.2021.100142>
- Napper IE, Thompson RC (2023) Plastics and the environment. *Annu Rev Environ Resour* 48(1):55–79. <https://doi.org/10.1146/annurev-environ-112522-072642>
- Schade A, Melzer M, Zimmermann S, Schwarz T, Stoeve K, Kuhn H (2024) Plastic waste recycling—a chemical recycling perspective. *ACS Sustain Chem Eng* 12(33):12270–12288. <https://doi.org/10.1021/acssuschemeng.4c02551>
- Ncube LK, Ude AU, Ogunmuyiwa EN, Zulkifli R, Beas IN (2020) Environmental impact of food packaging materials: a review of contemporary development from conventional plastics to polylactic acid based materials. *Materials* 13(21):4994. <https://doi.org/10.3390/ma13214994>
- IUCN-EA-QUANTIS (2020) National Guidance for plastic pollution hotspotting and shaping action, Country report Tanzania, vol 2021. [https://plastichotspotting.lifecycleinitiative.org/wp-content/uploads/2021/05/Tanzania\\_final\\_report\\_2021.pdf](https://plastichotspotting.lifecycleinitiative.org/wp-content/uploads/2021/05/Tanzania_final_report_2021.pdf)
- Abukhattala M, Fall M (2021) Geotechnical characterization of plastic waste materials in pavement subgrade applications. *Transp Geotech* 27:100472. <https://doi.org/10.1016/j.trgeo.2020.100472>
- Ahmed N (2023) Utilizing plastic waste in the building and construction industry: a pathway towards the circular economy. *Constr Build Mater* 383:131311. <https://doi.org/10.1016/j.conbuildmat.2023.131311>
- Wang C-Y, Chu H-Y, Wang C-C (2024) Converting waste PET plastics to high value-added MOFs-based functional materials: a state of the art review. *Coord Chem Rev* 518:216106. <https://doi.org/10.1016/j.ccr.2024.216106>
- Soong Y-HV, Sobkowicz MJ, Xie D (2022) Recent advances in biological recycling of Polyethylene Terephthalate (PET) plastic wastes. *Bioengineering* 9(3):98. <https://doi.org/10.3390/bioengineering9030098>
- Ávila F, Puertas E, Blanca-Hoyos Á, Ordóñez J (2024) Experimental evaluation of waste PET bottles as a sustainable building material. *J Archit Eng* 30(2):04024014. <https://doi.org/10.1061/AEIED.AEENG-1701>
- Lamba P, Kaur DP, Raj S, Sorout J (2022) Recycling/reuse of plastic waste as construction material for sustainable development: a review. *Environ Sci Pollut Res* 29(57):86156–86179. <https://doi.org/10.1007/s11356-021-16980-y>
- Ahmat T, Djomou Djonga PN, Hambate Gomdje V, Kamdoun Noukelack S (2021) Mechanical properties and chemical stability of bathroom wall composites manufactured from recycled polyethylene terephthalate (PET) mixed with cocoa hulls powder. *J Adv Chem Sci* 7(4):751–755. <https://doi.org/10.30799/jacs.243.21070402>
- Katariya M, Narulkar S (2023) A review of use of waste plastic as binder replacing cement in creation of construction elements. *Int J Innov Res Technol*
- Bamigboye GO, Ngene BU, Ademola D, Jolayemi JK (2019) Experimental study on the use of waste polyethylene terephthalate (PET) and River sand in roof tile production. *J Phys Conf Ser* 1378(4):042105. <https://doi.org/10.1088/1742-6596/1378/4/042105>
- Karedla AB, Schuster J, Shaik YP (2024) Possibility of making plastic roof tiles from waste plastic, sand, and fly ash. *Constr Mater* 4(3):597–610. <https://doi.org/10.3390/constrmater4030032>
- Mache E, Nthiga E, Muthakia GK (2023) Formulation and characterization of floor tile composite derived from Polyethylene Terephthalate waste and sand. Dedan Kimathi University of Technology Official Repository
- Laurian P, Chengula DH, Nyangi P (2024) The use of waste Polyethylene Terephthalate (PET) plastics for wall cladding materials in Mbeya Tanzania. *Eng Sci Technol J* 5(10):2897–2910. <https://doi.org/10.51594/estj.v5i10.1633>
- Naderi Kalali E, Lotfian S, Entezar Shabestari M, Khayatizadeh S, Zhao C, Yazdani Nezhad H (2023) A critical review of the current progress of plastic waste recycling technology in structural materials. *Curr Opin Green Sustain Chem* 40:100763. <https://doi.org/10.1016/j.cogsc.2023.100763>
- Xu J, Houndehou JD, Wang Z, Ma Q (2023) Experimental investigation on the mechanical properties and damage evolution of steel-fiber-reinforced crumb rubber concrete with porcelain tile waste. *Constr Build Mater* 370:130643. <https://doi.org/10.1016/j.conbuildmat.2023.130643>

20. Dalvand A, Ahmadi M (2021) Impact failure mechanism and mechanical characteristics of steel fiber reinforced self-compacting cementitious composites containing silica fume. *Eng Sci Technol Int J* 24(3):736–748. <https://doi.org/10.1016/j.jestch.2020.12.016>
21. Welî SS, Abbood IS, Hasan KF, Jasim MA (2020) Effect of steel fibers on the concrete strength grade: a review. *IOP Conf Ser Mater Sci Eng* 888(1):012043. <https://doi.org/10.1088/1757-899X/888/1/012043>
22. Merli R, Preziosi M, Acampora A, Lucchetti MC, Petrucci E (2020) Recycled fibers in reinforced concrete: a systematic literature review. *J Clean Prod* 248:119207. <https://doi.org/10.1016/j.jclepro.2019.119207>
23. Wu L, Li X, Deng H (2023) Flexural performance of hybrid fiber reinforced cement-based materials incorporating ceramic wastes. *Arch Civ Eng*. <https://doi.org/10.24425/ace.2023.146093>
24. Huo Y et al (2023) Dynamic tensile properties of steel fiber reinforced polyethylene fiber-engineered/strain-hardening cementitious composites (PE-ECC/SHCC) at high strain rate. *Cem Concr Compos* 143:105234. <https://doi.org/10.1016/j.cemconcomp.2023.105234>
25. Esmaeili J, Andalibi K, Gencel O (2021) Mechanical characteristics of experimental multi-scale steel fiber reinforced polymer concrete and optimization by Taguchi methods. *Constr Build Mater* 313:125500. <https://doi.org/10.1016/j.conbuildmat.2021.125500>
26. Zeybek Ö, Özkılıç YO, Çelik Aİ, Deifalla AF, Ahmad M, Sabri Sabri MM (2022) Performance evaluation of fiber-reinforced concrete produced with steel fibers extracted from waste tire. *Front Mater* 9:1057128. <https://doi.org/10.3389/fmats.2022.1057128>
27. Bayraktar OY, Kaplan G, Shi J, Benli A, Bodur B, Turkoglu M (2023) The effect of steel fiber aspect-ratio and content on the fresh, flexural, and mechanical performance of concrete made with recycled fine aggregate. *Constr Build Mater* 368:130497. <https://doi.org/10.1016/j.conbuildmat.2023.130497>
28. Zhang P, Wang C, Gao Z, Wang F (2023) A review on fracture properties of steel fiber reinforced concrete. *J Build Eng* 67:105975. <https://doi.org/10.1016/j.jobte.2023.105975>
29. Ammari MS, Belhadj B, Bederina M, Ferhat A, Quéneudec M (2020) Contribution of hybrid fibers on the improvement of sand concrete properties: barley straws treated with hot water and steel fibers. *Constr Build Mater* 233:117374. <https://doi.org/10.1016/j.conbuildmat.2019.117374>
30. Ji Y, Zhang H, Li W (2022) Investigation on steel fiber strengthening of waste brick aggregate cementitious composites. *Case Stud Constr Mater* 17:e01240. <https://doi.org/10.1016/j.cscm.2022.e01240>
31. Zhang P, Wang C, Wu C, Guo Y, Li Y, Guo J (2022) A review on the properties of concrete reinforced with recycled steel fiber from waste tires. *Rev Adv Mater Sci* 61(1):276–291. <https://doi.org/10.1515/rams-2022-0029>
32. Liew KM, Akbar A (2020) The recent progress of recycled steel fiber reinforced concrete. *Constr Build Mater* 232:117232. <https://doi.org/10.1016/j.conbuildmat.2019.117232>
33. Mendes JF, Castro LS, Corrêa AC, Marconcini JM, Mattoso LHC, Mendes RF (2021) Effects of short fibers and processing additives on HDPE composites properties reinforced with PINUS and EUCALYPTUS fibers. *J Appl Polym Sci* 138(15):50178. <https://doi.org/10.1002/app.50178>
34. Elhadary M, Hamdy A, Shaker W (2022) Effect of fiber bridging in composites healing. *Alex Eng J* 61(4):2769–2774. <https://doi.org/10.1016/j.aej.2021.08.002>
35. Li W et al (2021) Microstructure evolution and mechanical properties of 308L stainless steel coatings fabricated by laser hot wire cladding. *Mater Sci Eng A* 824:141825. <https://doi.org/10.1016/j.msea.2021.141825>
36. Guo C, Chen Y, Gao Y, Liu Y, Zhou Y, Wu J (2023) Enhancement of the tensile strength of Titanium/Aluminum triple-layer composite panels using steel fiber. *JOM* 75(8):2897–2908. <https://doi.org/10.1007/s11837-022-05600-w>
37. Chen Y et al (2022) Effect of the addition of steel fibers on the bonding interface and tensile properties of explosion-welded 2A12 aluminum alloy and SS-304 steel. *Materials* 16(1):116. <https://doi.org/10.3390/ma16010116>
38. Zanjani MMK, Peralta I, Fachinotti VD, Caggiano A (2024) Integrated structural and energy retrofitting based on cementitious composites and phase change materials. In: Banthia N, Soleimani-Dashtaki S, Mindess S (eds) *Smart & sustainable infrastructure: building a greener tomorrow*, vol 48, in RILEM Bookseries, vol. 48. Springer, Cham, pp 570–588. [https://doi.org/10.1007/978-3-031-53389-1\\_53](https://doi.org/10.1007/978-3-031-53389-1_53)
39. Schirmeister CG, Mülhaupt R (2022) Closing the carbon loop in the circular plastics economy. *Macromol Rapid Commun* 43(13):2200247. <https://doi.org/10.1002/marc.202200247>
40. Oladele IO, Omotosho TF, Adediran AA (2020) Polymer-based composites: an indispensable material for present and future applications. *Int J Polym Sci* 2020:1–12. <https://doi.org/10.1155/2020/8834518>
41. Chatziparaskeva G et al (2022) End-of-life of composite materials in the framework of the circular economy. *Microplastics* 1(3):377–392. <https://doi.org/10.3390/microplastics1030028>
42. M. of W. MoW (2000) *Laboratory testing manual*. Novum Grafisk AS, Skjetten Norway, Oslo. ISBN 9987-8891-3-1
43. Ismail AS, Jawaid M, Hamid NH, Yahaya R, Sain M, Sarmin SN (2022) Dimensional stability, density, void and mechanical properties of flax fabrics reinforced bio-phenolic/epoxy composites. *J Ind Text* 52:152808372211235. <https://doi.org/10.1177/15280837221123594>
44. Nikolić E, Delić-Nikolić I, Jovičić M, Miličić L, Mijatović N (2023) Recycling and reuse of building materials in a historical landscape—Viminacium Natural Brick (Serbia). *Sustainability* 15(3):2824. <https://doi.org/10.3390/su15032824>
45. Sivasakthi M, Jeyalakshmi R, Rajamane NP (2021) Fly ash geopolymer mortar: impact of the substitution of river sand by copper slag as a fine aggregate on its thermal resistance properties. *J Clean Prod* 279:123766. <https://doi.org/10.1016/j.jclepro.2020.123766>
46. Yön MŞ, Arslan F, Karatas M, Benli A (2022) High-temperature and abrasion resistance of self-compacting mortars incorporating binary and ternary blends of silica fume and slag. *Constr Build Mater* 355:129244. <https://doi.org/10.1016/j.conbuildmat.2022.129244>
47. Nor Arman NS, Chen RS, Ahmad S (2021) Review of state-of-the-art studies on the water absorption capacity of agricultural fiber-reinforced polymer composites for sustainable construction. *Constr Build Mater* 302:124174. <https://doi.org/10.1016/j.conbuildmat.2021.124174>
48. Kumavat HR, Chandak NR, Patil IT (2021) Factors influencing the performance of rebound hammer used for non-destructive testing of concrete members: a review. *Case Stud Constr Mater* 14:e00491. <https://doi.org/10.1016/j.cscm.2021.e00491>
49. Li H, Li X, Fu J, Gao Z, Chen P, Zhang Z (2023) Research on acoustic emission multi-parameter characteristics in the failure process of imitation steel fiber reinforced concrete. *Phys Fluids*. <https://doi.org/10.1063/5.0170179>
50. Takahashi K, Yamamoto K, Kuchiba A, Koyama T (2022) Confidence interval for micro-averaged F1 and macro-averaged F1 scores. *Appl Intell* 52(5):4961–4972. <https://doi.org/10.1007/s10489-021-02635-5>

51. Lika K, Kooijman SALM (2024) The relationship between confidence intervals and distributions of estimators for parameters of deterministic models. *Ecol Model* 490:110645. <https://doi.org/10.1016/j.ecolmodel.2024.110645>
52. Prasetya Aji M, Rahmawati I, Priyanto A, Marwoto P (2023) Novel one-step synthesis of solid-state carbonized polymer dots by heating at around melting point of polyethylene terephthalate (PET) bottle plastic waste. *Environ Nanotechnol Monit Manag* 20:100892. <https://doi.org/10.1016/j.enmm.2023.100892>
53. Celik Y, Shamsuyeva M, Endres HJ (2022) Thermal and mechanical properties of the recycled and virgin PET—Part I. *Polymers* 14(7):1326. <https://doi.org/10.3390/polym14071326>
54. Ciobanu RC et al (2023) Special packaging materials from recycled PET and metallic nano-powders. *Polymers* 15(15):3161. <https://doi.org/10.3390/polym15153161>
55. C21 Committee. Test Methods for Determination of Water Absorption and Associated Properties by Vacuum Method for Pressed Ceramic Tiles and Glass Tiles and Boil Method for Extruded Ceramic Tiles and Non-tile Fired Ceramic Whiteware Products. <https://doi.org/10.1520/C0373-18>
56. C21 Committee. Test Method for Determination of Breaking Strength and Modulus of Rupture of Ceramic Tiles and Glass Tiles by Three-Point Loading. <https://doi.org/10.1520/C1505-15R22>
57. Sayı CÖ, Eren Ö (2022) Physical and durability properties of recycled polyethylene terephthalate (PET) fibre reinforced concrete. *Eur J Environ Civ Eng* 26(14):7084–7102. <https://doi.org/10.1080/19648189.2021.1976681>
58. Singh AK, Bedi R, Kaith BS (2021) Composite materials based on recycled polyethylene terephthalate and their properties—a comprehensive review. *Compos Part B Eng* 219:108928. <https://doi.org/10.1016/j.compositesb.2021.108928>
59. Hasanzadeh A, Shooshpasha I (2023) PET fiber reinforcement efficiency in the mechanical and microstructural characteristics of cemented sand modified with silica fume. *Constr Build Mater* 397:132363. <https://doi.org/10.1016/j.conbuildmat.2023.132363>

**Publisher's Note** Springer Nature remains neutral with regard to jurisdictional claims in published maps and institutional affiliations.

Springer Nature or its licensor (e.g. a society or other partner) holds exclusive rights to this article under a publishing agreement with the author(s) or other rightsholder(s); author self-archiving of the accepted manuscript version of this article is solely governed by the terms of such publishing agreement and applicable law.